JOURNAL OF MOLECULAR SPECTROSCOPY **192,** 25–31 (1998)
ARTICLE NO. MS987651

Millimeter and Submillimeter-Wave Spectrum of Hydrogen Peroxide in the Ground and $v_3 = 1$ Vibrational States

Douglas T. Petkie,*,[1] Thomas M. Goyette,*,[2] Frank C. De Lucia,* Paul Helminger,†
S. P. Belov,‡ and G. Winnewisser‡

*Department of Physics, The Ohio State University, Columbus, Ohio 43210; †Department of Physics, University of South Alabama, Mobile, Alabama 36688; and ‡I. Physikalisches Institut, Universitat zu Koln, D-50937 Koln, Germany

Received April 1, 1998; in revised form June 2, 1998

The first measurements of the millimeter- and submillimeter (mm/submm)-wave rotational–torsional transitions in the $v_3 = 1$ ground torsional state ($n = 0$) of hydrogen peroxide are reported. The 149 newly measured transitions extend from 72 to 623 GHz in frequency and up to $J = 32$ and $K_a = 3$ in rotational quantum number. Additional measurements in the ground vibrational and torsional state around 1 THz are also reported. These data, along with all previously published microwave, mm/submm-wave, and far infrared data in the ground and $v_3 = 1$ vibrational state, along with recent infrared measurements, have been fitted simultaneously to their respective experimental uncertainties using a multi-state Hamiltonian that includes Fermi- and Coriolis-type interactions.

I. INTRODUCTION

Hydrogen peroxide (HOOH) is the simplest molecule which undergoes internal rotation, and it has been extensively studied in the microwave (mw), millimeter/submillimeter (mm/submm), far infrared (fir), and infrared (ir). This work has been motivated by fundamental interest in its complex rotation–torsion–vibration spectrum and the role it plays in upper atmospheric chemistry. Its spectroscopy has been discussed in some detail by Petkie *et al.* (*1*) and by Camy-Peyret *et al.* (*2*).

Figure 1 shows the torsional potential function for HOOH and the labeling of levels. The torsional motion of the two O–H bonds relative to one another about the O–O bond leads to a set of four torsional levels, $\tau = 1, 2, 3, 4$ in order of ascending energy, within each fundamental torsional state n. The low *trans* barrier to internal rotation ($\sim 387\ cm^{-1}$) leads to a splitting between $\tau = 1, 2$ and $\tau = 3, 4$ levels, with each pair of levels containing a complete set of rotational levels. The larger *cis* barrier ($\sim 2563\ cm^{-1}$) can lead to a splitting between the pairs of torsional levels that results in a "staggering" of the even and odd K_a rotational energy levels. HOOH also has a cascading set of $\Delta K_a = \pm 2$ Fermi resonance interactions that connect the torsional levels $(n, \tau) \leftrightarrow (n \pm 1, \tau)$. Additionally, there exists a Coriolis interaction between the $v_3 = 1, n = 0(1)$, and ground vibrational ($v = 0$) $n = 2(3)$ states that couples torsional levels of different symmetry, namely $\tau = 1 \leftrightarrow 2$ and $3 \leftrightarrow 4$. The Fermi and Coriolis interactions quickly lead to a large multi-state Hamiltonian matrix coupling the $v = 0$ torsional states with those of $v_3 = 1$.

Interestingly, the analysis technique for the treatment of the torsional problem which has evolved is largely empirical. Helminger *et al.* (*3*) showed that the high-resolution rotation–torsional spectrum in the mm/submm could be described by using a Watson Hamiltonian with one set of constants for the lower ($\tau = 1, 2$) and another for the upper ($\tau = 3, 4$) torsional sublevels of the $n = 0$ torsional state. The only manifestation of the torsion was an $\sim 11.5\ cm^{-1}$ splitting between these two

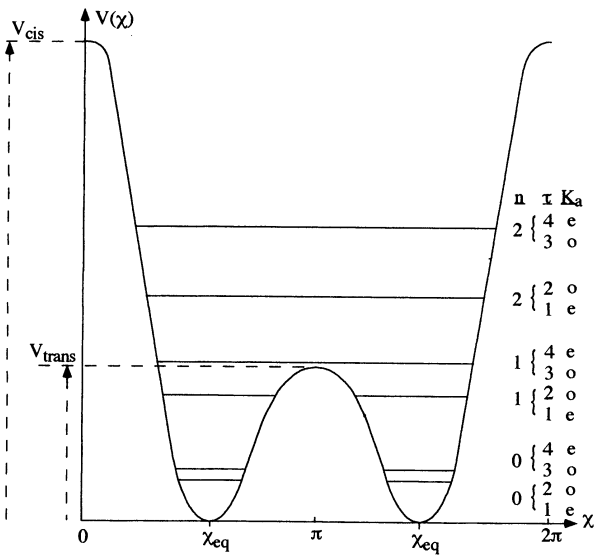

FIG. 1. The torsional potential function of HOOH. Note the rotational energy level distribution due to the rotational–torsional symmetry considerations. The splittings shown are not to scale.

[1] Current address: Science Department, Bluffton College, Bluffton, OH 45817.

[2] Current address: University of Massachusetts at Lowell, Department of Physics, Lowell, MA 01854.

0022-2852/98 $25.00

TABLE 1—*Continued*

$\tau = 3, 4$[a]				$\tau = 1, 2$					$\tau = 3, 4$[a]				$\tau = 1, 2$				
J'	K'_a	K'_c		J''	K''_a	K''_c	ν_{obs}(MHz)	o-c[b]	J'	K'_a	K'_c		J''	K''_a	K''_c	ν_{obs}(MHz)	o-c[b]
21	1	20	→	21	2	20	351252.312	136	13	2	12	←	14	1	14	538372.240	172
24	1	23	→	24	2	23	316894.050	12	14	2	13	←	15	1	15	496763.990	70
10	2	9	→	9	3	7	512448.590	93	15	2	14	←	16	1	16	455820.264	46
12	2	11	→	11	3	9	410674.144	-20	16	2	15	←	17	1	17	415550.645	15
13	2	12	→	12	3	10	359820.288	-23	17	2	16	←	18	1	18	375965.025	-69
14	2	13	→	13	3	11	309001.435	-90	18	2	17	←	19	1	19	337073.724	-70
15	2	14	→	14	3	12	258228.040	-18	19	2	18	←	20	1	20	298887.030	-96
17	2	16	→	16	3	14	156860.435	77	22	2	21	←	23	1	23	188661.396	-52
22	2	21	←	21	3	19	94967.386	-23	23	2	22	←	24	1	24	153400.456	-25
23	2	22	←	22	3	20	144960.859	155	24	2	23	←	25	1	25	118898.287	22
10	2	8	→	9	3	6	511323.390	-48	32	2	31	→	33	1	33	128486.793	7
11	2	9	→	10	3	7	459930.720	75	12	2	10	←	13	1	12	484943.440	-164
12	2	10	→	11	3	8	408406.390	-12	13	2	11	←	14	1	13	428443.360	-144
13	2	11	→	12	3	9	356734.224	23	14	2	12	←	15	1	14	371732.560	-57
15	2	13	→	14	3	11	252874.178	-10	15	2	13	←	16	1	15	314853.008	42
17	2	15	→	16	3	13	148197.894	69	16	2	14	←	17	1	16	257849.168	73
22	2	20	←	21	3	18	118142.087	-19	18	2	16	←	19	1	18	143658.842	147
23	2	21	←	22	3	19	172369.239	68	23	2	21	→	24	1	23	140452.737	50
11	2	10	←	12	1	12	623544.570	15	27	2	25	→	28	1	27	362613.327	9

[a] K'_a odd indicates a transition between $\tau = 3 \leftrightarrow 1$ while K'_a even indicates a transition between $\tau = 4 \leftrightarrow 2$.
[b] Observed minus calculated differences are reported in units of kHz.

combined these new data with the mm/submm data (*3, 7, 8*) and ir data (*2*) in a new analysis.

In this paper, for our analysis we adopt the multi-state interaction scheme of Camy-Peyret, *et al.* (*2*) because the $v_3 = 1$, $n = 0$ mm/submm-wave transitions (specifically the $\tau = 3$, 4 rotational–torsional levels) are perturbed by a strong Coriolis interaction with the $v = 0$, $n = 2$, $\tau = 3$, 4 levels. Because of the cascading interactions, we include all published relevant data, including our earlier mm/submm data as summarized in Petkie *et al.* (*1*), the fir data of Bellini *et al.* (*4*), and the ir work of Olson *et al.* (*5*) and Camy-Peyret *et al.* (*2*) along with our new measurements of rotation–torsional transitions within the $n = 0$ torsional level of the $v_3 = 1$ vibrational state and measurements of the $^rQ_2$ branch in the $n = 0$ torsional level of the ground vibrational state.

II. EXPERIMENTAL DETAILS

Our experimental techniques have been discussed previously and only a brief summary will be presented here. Three mm/submm-wave spectrometers were used and differed significantly only in their generation of the mm/submm-wave radiation. In the first, the output of a phased-locked 10–15 GHz voltage tunable YIG oscillator was tripled and amplified by a Traveling Wave Tube Amplifier and matched onto a harmonic generator in order to generate radiation in the 100–700 GHz region (*9*). The second source was a commercial 118-178 GHz Kvartz synthesizer based on a phased-locked ISTOK OB-86 backward-wave oscillator. The measurements around 1 THz were made with an ISTOK BWO which was phase locked to a Kvartz synthesizer (*10*). Typically, the mm/submm-wave power was quasi-optically propagated through a 6-ft-long, 6-in-diameter glass absorption cell sealed with Teflon windows and detected by either a liquid ^{4}He-cooled InSb hot electron bolometer or a liquid ^{3}He-cooled Si bolometer. The cell pressure was maintained near 20 mTorr, which led to lines dominated by Doppler broadening. Because hydrogen peroxide decomposes quickly, especially on metallic surfaces, a continuous flow of vapor from a 70% solution of hydrogen peroxide (obtained from DuPont Chemicals) was maintained. The $n = 0$, $v_3 = 1$ vibrational band is near 866 cm^{-1}, which results in ~1.5% population at 300 K. Because of strong absorption in the mm/submm region and the sparse spectrum of HOOH, this population was sufficient for this work. The experimental uncertainty of the measured frequencies is estimated to be <100 kHz.

III. ANALYSIS

To keep the literature as consistent as possible, we have used the distortion and interaction Hamiltonian terms of Camy-Peyret *et al.* (*2*) and Petkie *et al.* (*1*) as our starting point for our selection of the final Hamiltonian used to describe the global data set. We have also chosen to do our analysis in the context of the generally available and well documented asymmetric rotor program CALFIT (*11*) so that our results, which unify the global ir-mm/submm data set, are in a form readily available to the several communities involved in this work. The mm/submm-wave and ir data were weighted according to the inverse square of their experimental uncertainties, ~0.10 and ~15 MHz, respectively.

The most significant difference between our Hamiltonian

TABLE 1—*Continued*

$\tau = 3, 4^a$				$\tau = 1, 2$					$\tau = 3, 4^a$				$\tau = 1, 2$				
J'	K'_a	K'_c		J''	K''_a	K''_c	ν_{obs}(MHz)	o-c[b]	J'	K'_a	K'_c		J''	K''_a	K''_c	ν_{obs}(MHz)	o-c[b]
21	1	20	→	21	2	20	351252.312	136	13	2	12	←	14	1	14	538372.240	172
24	1	23	→	24	2	23	316894.050	12	14	2	13	←	15	1	15	496763.990	70
10	2	9	→	9	3	7	512448.590	93	15	2	14	←	16	1	16	455820.264	46
12	2	11	→	11	3	9	410674.144	-20	16	2	15	←	17	1	17	415550.645	15
13	2	12	→	12	3	10	359820.288	-23	17	2	16	←	18	1	18	375965.025	-69
14	2	13	→	13	3	11	309001.435	-90	18	2	17	←	19	1	19	337073.724	-70
15	2	14	→	14	3	12	258228.040	-18	19	2	18	←	20	1	20	298887.030	-96
17	2	16	→	16	3	14	156860.435	77	22	2	21	←	23	1	23	188661.396	-52
22	2	21	←	21	3	19	94967.386	-23	23	2	22	←	24	1	24	153400.456	-25
23	2	22	←	22	3	20	144960.859	155	24	2	23	←	25	1	25	118898.287	22
10	2	8	→	9	3	6	511323.390	-48	32	2	31	→	33	1	33	128486.793	7
11	2	9	→	10	3	7	459930.720	75	12	2	10	←	13	1	12	484943.440	-164
12	2	10	→	11	3	8	408406.390	-12	13	2	11	←	14	1	13	428443.360	-144
13	2	11	→	12	3	9	356734.224	23	14	2	12	←	15	1	14	371732.560	-57
15	2	13	→	14	3	11	252874.178	-10	15	2	13	←	16	1	15	314853.008	42
17	2	15	→	16	3	13	148197.894	69	16	2	14	←	17	1	16	257849.168	73
22	2	20	←	21	3	18	118142.087	-19	18	2	16	←	19	1	18	143658.842	147
23	2	21	←	22	3	19	172369.239	68	23	2	21	→	24	1	23	140452.737	50
11	2	10	←	12	1	12	623544.570	15	27	2	25	→	28	1	27	362613.327	9

[a] K'_a odd indicates a transition between $\tau = 3 \leftrightarrow 1$ while K'_a even indicates a transition between $\tau = 4 \leftrightarrow 2$.
[b] Observed minus calculated differences are reported in units of kHz.

combined these new data with the mm/submm data (*3, 7, 8*) and ir data (*2*) in a new analysis.

In this paper, for our analysis we adopt the multi-state interaction scheme of Camy-Peyret, *et al.* (*2*) because the $v_3 = 1$, $n = 0$ mm/submm-wave transitions (specifically the $\tau = 3$, 4 rotational–torsional levels) are perturbed by a strong Coriolis interaction with the $v = 0$, $n = 2$, $\tau = 3$, 4 levels. Because of the cascading interactions, we include all published relevant data, including our earlier mm/submm data as summarized in Petkie *et al.* (*1*), the fir data of Bellini *et al.* (*4*), and the ir work of Olson *et al.* (*5*) and Camy-Peyret *et al.* (*2*) along with our new measurements of rotation–torsional transitions within the $n = 0$ torsional level of the $v_3 = 1$ vibrational state and measurements of the $^rQ_2$ branch in the $n = 0$ torsional level of the ground vibrational state.

II. EXPERIMENTAL DETAILS

Our experimental techniques have been discussed previously and only a brief summary will be presented here. Three mm/submm-wave spectrometers were used and differed significantly only in their generation of the mm/submm-wave radiation. In the first, the output of a phased-locked 10–15 GHz voltage tunable YIG oscillator was tripled and amplified by a Traveling Wave Tube Amplifier and matched onto a harmonic generator in order to generate radiation in the 100–700 GHz region (*9*). The second source was a commercial 118-178 GHz Kvartz synthesizer based on a phased-locked ISTOK OB-86 backward-wave oscillator. The measurements around 1 THz were made with an ISTOK BWO which was phase locked to a Kvartz synthesizer (*10*). Typically, the mm/submm-wave power was quasi-optically propagated through a 6-ft-long, 6-in-diameter glass absorption cell sealed with Teflon windows and detected by either a liquid ^{4}He-cooled InSb hot electron bolometer or a liquid ^{3}He-cooled Si bolometer. The cell pressure was maintained near 20 mTorr, which led to lines dominated by Doppler broadening. Because hydrogen peroxide decomposes quickly, especially on metallic surfaces, a continuous flow of vapor from a 70% solution of hydrogen peroxide (obtained from DuPont Chemicals) was maintained. The $n = 0$, $v_3 = 1$ vibrational band is near 866 cm^{-1}, which results in ~1.5% population at 300 K. Because of strong absorption in the mm/submm region and the sparse spectrum of HOOH, this population was sufficient for this work. The experimental uncertainty of the measured frequencies is estimated to be <100 kHz.

III. ANALYSIS

To keep the literature as consistent as possible, we have used the distortion and interaction Hamiltonian terms of Camy-Peyret *et al.* (*2*) and Petkie *et al.* (*1*) as our starting point for our selection of the final Hamiltonian used to describe the global data set. We have also chosen to do our analysis in the context of the generally available and well documented asymmetric rotor program CALFIT (*11*) so that our results, which unify the global ir-mm/submm data set, are in a form readily available to the several communities involved in this work. The mm/submm-wave and ir data were weighted according to the inverse square of their experimental uncertainties, ~0.10 and ~15 MHz, respectively.

The most significant difference between our Hamiltonian

TABLE 2
Newly Observed Millimeter/Submillimeter-Wave Transitions in the $n = 0$ and $n = 1$ Torsional States of the Ground Vibrational State

$\tau = 3, 4$[a]				$\tau = 1, 2$							$\tau = 3, 4$[a]				$\tau = 1, 2$						
J'	K'_a	K'_c		J''	K''_a	K''_c	n	ν_{obs}(MHz)[b]	o-c[c]	unc[c]	J'	K'_a	K'_c		J''	K''_a	K''_c	n	ν_{obs}(MHz)[b]	o-c[c]	unc[c]
24	1	24	←	23	2	22	0	607679.040	-15	100	29	2	28	→	29	3	26	0	1042579.580	297	150
21	3	19	←	22	2	21	0	607718.600	69	100	3	2	1	→	3	3	1	0	1038378.911	7	50
9	1	9	→	10	2	9	0	1018030.411	-17	50	4	2	2	→	4	3	2	0	1038192.160	0	30
10	1	9	→	11	2	9	0	1023757.742	52	50	5	2	3	→	5	3	3	0	1037946.459	2	30
13	3	11	←	14	2	13	0	1006256.092	9	50	6	2	4	→	6	3	4	0	1037633.597	1	50
11	3	9	→	10	4	7	0	1024498.181	23	50	7	2	5	→	7	3	5	0	1037243.554	-172	50
11	3	8	→	10	4	6	0	1024489.152	9	50	8	2	6	→	8	3	6	0	1036765.328	-17	50
49	0	49	←	49	1	49	0	490270.270	88	100	9	2	7	→	9	3	7	0	1036185.292	-9	50
50	0	50	←	50	1	50	0	502233.760	-104	100	10	2	8	→	10	3	8	0	1035488.785	-18	30
31	4	27	→	30	5	25	0	533483.825	113	100	11	2	9	→	11	3	9	0	1034659.428	-12	30
31	4	28	→	30	5	26	0	533490.230	105	100	12	2	10	→	12	3	10	0	1033679.202	-12	50
33	4	30	→	32	5	28	0	427963.400	-36	100	13	2	11	→	13	3	11	0	1032528.578	-6	50
36	4	32	→	35	5	30	0	269106.940	-252	100	14	2	12	→	14	3	12	0	1031186.540	16	100
38	4	35	→	37	5	33	0	162376.031	132	100	15	2	13	→	15	3	13	0	1029630.618	7	50
39	4	36	→	38	5	34	0	108805.388	-103	100	16	2	14	→	16	3	14	0	1027837.120	-2	50
3	2	2	→	3	3	0	0	1038390.321	5	50	17	2	15	→	17	3	15	0	1025781.163	-3	50
4	2	3	→	4	3	1	0	1038226.423	9	30	18	2	16	→	18	3	16	0	1023436.822	-8	50
5	2	4	→	5	3	2	0	1038026.430	0	30	19	2	17	→	19	3	17	0	1020777.385	20	100
6	2	5	→	6	3	3	0	1037793.648	-4	30	20	2	18	→	20	3	18	0	1017775.359	-24	50
7	2	6	→	7	3	4	0	1037532.043	-7	50	21	2	19	→	21	3	19	0	1014403.061	-28	50
8	2	7	→	8	3	5	0	1037246.415	127	50	22	2	20	→	22	3	20	0	1010632.513	-18	50
9	2	8	→	9	3	6	0	1036941.729	-17	50	23	2	21	→	23	3	21	0	1006435.877	10	50
10	2	9	→	10	3	7	0	1036624.515	-15	50	23	2	22	←	23	1	22	0	1035248.933	-55	30
11	2	10	→	11	3	8	0	1036301.493	-7	50	24	2	23	←	24	1	23	0	1024219.173	-40	50
12	2	11	→	12	3	9	0	1035980.274	-13	50	25	2	24	←	25	1	24	0	1012859.497	3	50
13	2	12	→	13	3	10	0	1035669.324	0	30	26	2	25	←	26	1	25	0	1001188.439	128	50
14	2	13	→	14	3	11	0	1035377.878	10	30	2	2	1	←	3	1	3	0	1019529.143	11	50
15	2	14	→	15	3	12	0	1035116.046	11	50	18	0	18	→	19	1	18	0	1008541.366	-18	50
16	2	15	→	16	3	13	0	1034894.841	11	50	21	0	21	←	20	1	19	0	1020702.893	16	50
17	2	16	→	17	3	14	0	1034726.206	26	50	23	4	19	←	24	3	21	0	1044121.136	-400	200
18	2	17	→	18	3	15	0	1034622.994	19	30	30	2	29	←	31	3	29	1	541938.640	-9	100
19	2	18	→	19	3	16	0	1034599.112	9	30	27	3	24	←	28	4	24	1	157254.856	38	100
20	2	19	→	20	3	17	0	1034669.495	2	30	33	3	30	→	34	4	30	1	131375.382	-49	100
21	2	20	→	21	3	18	0	1034850.117	-39	50	33	3	31	→	34	4	31	1	135916.270	-21	100
22	2	21	→	22	3	19	0	1035158.207	-23	50	34	3	31	→	35	4	31	1	179257.080	42	100
23	2	22	→	23	3	20	0	1035611.995	-29	30	10	5	5	←	10	6	5	1	434118.950	289	100
24	2	23	→	24	3	21	0	1036231.028	-36	50	5	5	1	←	6	6	1	1	122370.625[d]	222	100
25	2	24	→	25	3	22	0	1037036.101	-39	50	9	6	3	←	8	7	1	1	328589.186[d]	-40	100
26	2	25	→	26	3	23	0	1038049.321	-28	30	13	6	7	←	12	7	5	1	537885.680[d]	94	100
27	2	26	→	27	3	24	0	1039294.128	-12	30	17	6	11	→	18	7	11	1	1030405.416[d]	-62	100
28	2	27	→	28	3	25	0	1040795.392	33	30	21	2	19	←	22	3	19	1	1013983.103	-2	50

[a] K'_a odd indicates a transition between $\tau = 3 \leftrightarrow 1$ while K'_a even indicates a transition between $\tau = 4 \leftrightarrow 2$.
[b] Frequencies greater than 1 THz were measured at the Universitat zu Koln.
[c] Observed minus calculated differences and the line position uncertainties are given in units of kHz.
[d] The transition with the larger statistical weight is reported for unresolved K-doublet transitions.

and that of Camy-Peyret *et al.* is that the inclusion of the high accuracy mm/submm data makes possible the observation of separate spectral parameters in $n = 0$ and $n = 1$ in the ground vibrational state, as well as the determination of higher order centrifugal distortion parameters.

For the $v_3 = 1$ vibrational state, energy levels from Ref. (2) were used as a starting point for initial assignments. Subsequent assignments were made by following smooth difference plots in each rotational branch. Initially, as the mm/submm-wave data were measured they were included in a "truncated" analysis which combined them with a limited set of $v_3 = 1$, $n = 0$ ir data ($K_a < 4$), which excluded the highly perturbed levels. Only a Coriolis interaction with a fixed set of rotational constants for the interacting state ($n = 2$, $\tau = 4$ ground vibrational state) was needed to fit the mm/submm-wave transitions to their experimental accuracy. This analysis, while useful for assignment and bootstrapping purposes, had little predictive power for the mm/submm spectrum outside of the limited range of the data set. For the ${}^rQ_2$ branch of the ground state our earlier mm/submm analysis was used to provide the initial search parameters.

IV. RESULTS

Tables 1 and 2 show the newly observed mm/submm transitions, and the spectral constants which result from our fits are shown in Tables 3 and 4. Although in analyses with many highly correlated constants it is ordinarily not too profitable to make comparisons between constants derived from analyses which use different choices of Hamiltonian constants and which analyze different data sets, a few useful observations are possible. First, there is clearly a strong mapping between this

TABLE 3

Rovibrational and Interaction Constants[a] for the τ = 1, 2 Torsional Levels

Rotational Constants	n = 0, τ = 1	n = 0, τ = 2	n = 1, τ = 1	n = 1, τ = 2	n = 2, τ = 1[c] n = 2, τ = 2	n = 3, τ = 1[c] n = 3, τ = 2	ν_3 = 1, n = 0, τ = 1, 2[c]	ν_3 = 1, n = 1, τ = 1, 2[b,c]
E (cm^{-1})			254.549586(87)	254.5502577(947)	569.74288(10) 569.74447(11)	1000.8819(1) 1000.9305(1)	865.9390582(306)	1117.248(27)
A	301874.2654(91)	301874.2622(247)	301251.1129(2124)	301249.4552(2499)	298809.46(22)	296496.51(36) 296490.6(5)	301285.120(26)	300661.9
B	26194.08965(206)	26190.46744(2437)	26271.62025(8767)	26273.66016(7813)	25982.038(172)	25708.09(19) 25724.76(11)	25870.72122(32377)	25879.9
C	25116.88435(146)	25120.50894(2424)	24836.83568(8846)	24834.57973(7950)	25154.716(198)	25341.27(18) 25324.92(10)	24774.38483(32198)	24484.05
Δ_J ×10^2	9.0470263(2527)	8.7127754(20612)	8.9050081(25477)	9.223150(6076)	8.9267(79)	9.7001(91) 9.5195(86)	9.867625(27295)	
Δ_{JK}	1.178589(90)	1.191749(96)	1.153544(451)	1.138685(641)	1.1348(5)	1.0752(9) 1.1108(14)	1.12916(119)	
Δ_K ×10^1	1.200467(113)	1.198975(280)	1.154130(519)	1.150127(626)	1.07903(53)	1.0210(5) 1.0188(10)	1.1945(4)	
δ_J ×10^3	-0.441964(1567)	-0.481137(4165)	4.3875(748)	4.4999(409)	3.931(57)		-0.2631(52)	
δ_K	0.591486(341)	-1.227015(12112)	0.36152(1389)	1.42271(3272)	1.460(89)	-2.835(52)	4.906327(161557)	
H_J ×10^7	-1.77362(1975)	-2.10153(5583)	2.4309(1058)	3.9376(5040)			0.98404(13068)	
H_{JK} ×10^5	0.42540(1404)	0.96170(1906)	0.82455(3518)	1.0605(1136)			6.9596(6621)	
H_{KJ} ×10^4	0.6472(361)	0.7292(486)	1.1857(573)	1.2512(721)			-4.281(531)	
H_K ×10^2	0.21460(461)	0.1966(49)	0.18759(377)	0.13402(427)	0.1341(30)		0.201(16)	
h_J ×10^7	-1.29829(1499)	-2.29275(3130)	0.8390(3834)					
h_{JK} ×10^4		-0.498688(37186)		2.2360(2794)	4.27(50)		1.2627(489)	
L_J ×10^{10}	0.26552(453)							
L_{JJK} ×10^8		0.26014(1390)		0.43150(9432)				
L_{JK} ×10^7	-0.1411(445)	-0.5935(477)						
L_K ×10^6	-1.88(36)	-0.827(284)						
l_J ×10^{11}	0.56923(3968)	1.3799(725)						
l_{JK} ×10^8	2.4286(270)	4.16627(22663)						

Interaction Constants	n = 0 ↔ 1, τ = 1	n = 0 ↔ 1, τ = 2	n = 1 ↔ 2, τ = 1	n = 1 ↔ 2, τ = 2	n = 2 ↔ 3, τ = 1 n = 2 ↔ 3, τ = 2	ν_3 =1: n = 0 ↔ 1, τ = 1 ν_3 =1: n = 0 ↔ 1, τ = 2	
W	166.26846(360)	186.99127(9894)	192.9612(287)	193.4371(446)	208.69(72) 209.55(71)	116.222(2150) 115.643(2152)	
W_J ×10^3	-2.01602(431)	-2.62369(1622)					
W_K		-0.421141(2063)					
C						n = 3, τ = 1 ↔ ν_3 =1, n = 1, τ = 2 n = 3, τ = 2 ↔ ν_3 =1, n = 1, τ = 1	323.26(29) 285.20(143)

[a] All constants are in units of MHz except where indicated. The uncertainties in parenthesis are one standard deviation and refer to the least significant digits. Enough digits are supplied to reproduce the observed spectra.

[b] Constants without uncertainties were constained to the values reported by Ref. 2.

[c] When only one value appears, the constants for the τ = 1 and 2 torsional states were constrained to be equal.

analysis and that of Camy-Peyret *et al.* because both reproduce the infrared data set equally well. Table 5 shows in more detail the quality of our fit to each of the data sets. The analysis of Ref. (*2*) of the infrared data set alone yielded rms deviations of 0.00083 and 0.00049 cm^{-1} for the τ = 1, 2 and τ = 3, 4 states, respectively. These are essentially identical with the results of our fits. The fits to the other data sets are also shown in Table 5. Again, the residuals are consistent with the expected experimental uncertainty and earlier more restrictive analyses.

In general the agreement between the parameters is as expected, with the lower order terms in good agreement (within a few standard deviations) and with ever larger differences at higher order where the combination of different data, different Hamiltonians, and correlation among spectral constants can lead to significantly different values for the parameters. In the analysis of this work, the parameters which are most directly linked to the mm/submm data set have significantly higher accuracy. This is especially true for the n = 0 states for which there are extensive data sets. The differences between the two analyses are largest (relative to the uncertainties of the analysis of Camy-Peyret *et al.*) where there is little or no first order data and the parameters are determined primarily through their interactions with directly observed states. This effect is largest in τ = 3, 4 and can be traced to correlations with the Fermi interaction parameters. Specifically, the W interaction parameters connecting the ground state $n = 2 \leftrightarrow n = 3$, τ = 3, 4 states are significantly different from those of Ref. (*2*) where the corresponding parameters are $h_{033.023}$ and $h_{034.024}$. Note that these parameters are defined differently in this paper (and Ref. *1*) compared to Ref. (*2*) with $W = h/2$. These, which differ by

TABLE 4

Rovibrational and Interaction Constants[a] for the $\tau = 3, 4$ Torsional Levels

Rotational Constants		$n = 0, \tau = 3$	$n = 0, \tau = 4$	$n = 1, \tau = 3$	$n = 1, \tau = 4$	$n = 2, \tau = 3$[c] $n = 2, \tau = 4$	$n = 3, \tau = 3, 4$[b]	$\nu_3 = 1, n = 0, \tau = 3, 4$[c]
E (cm^{-1})		11.437287(2)	11.4372963(11)	370.8933335(677)	370.8932899(1036)	776.11272(13) 776.12209(12)	1235.	877.9344760(306)
A		301586.4348(463)	301586.2713(99)	299838.6265(1767)	299839.8812(3019)	297590.81(41) 297590.20(41)	295400.	300999.696(63)
B		26142.72516(101)	26142.74724(213)	26054.06352(12098)	26055.27973(16477)	25862.465(970) 25862.77(97)	25710.	25820.71926(13140)
C		25199.33078(96)	25199.32283(202)	25144.64949(12031)	25143.35834(17291)	25244.185(976) 25243.851(975)	25300.	24859.40805(13092)
Δ_J	$\times 10^1$	0.89169942(2535)	0.89209143(4465)	0.88235065(82423)	0.8899591(8596)	0.95936(449)		1.0018127(1269)
Δ_{JK}		1.196443(96)	1.196235(111)	1.162458(745)	1.160599(727)	1.0945(23)		1.13546(78)
Δ_K	$\times 10^1$	1.186432(614)	1.184440(115)	1.113234(455)	1.115992(854)	1.0513(11)		1.2896(27)
δ_J	$\times 10^3$	0.563000(371)	0.720856(13576)	2.3257(196)	2.3319(580)	2.227(22)		0.92812(1199)
δ_K				-0.21248(5677)	0.40557(6549)	8.3375(4855)		4.28614(76768)
H_J	$\times 10^7$	-2.07766(2007)	1.15979(21435)	3.0904(983)				1.4616(1727)
H_{JK}	$\times 10^6$	5.7718(1270)	0.6232(3006)	8.8712(8744)	-16.624(2114)	358.3(436)		-579.241(27770)
H_{KJ}	$\times 10^4$	1.1420(301)	1.3544(442)	1.3665(1033)	3.0673(1464)	-12.13(152)		16.12(275)
H_K	$\times 10^2$	0.25283(2281)	0.18398(188)	0.12777(281)	0.11344(696)	0.1890(136)		6.914(182)
h_J	$\times 10^7$	-0.36796(286)	-0.529545(13263)					-0.3802(1282)
h_{JK}	$\times 10^4$		1.50973(13513)	1.2837(742)	1.1471(2893)			1.8779(1145)
h_K	$\times 10^3$				-9.5718(9029)			-352.874(11308)
L_J	$\times 10^{11}$	-3.42918(23092)						7.896(1016)
L_{JJK}	$\times 10^9$	-0.6324(257)	4.6131(2014)					-27.652(2236)
L_{JK}	$\times 10^8$	-3.198(276)	-1.478(313)	-3.840(1345)				6305.54(27283)
L_{JKK}	$\times 10^7$	2.13(39)	-4.119(681)					-1786.(112)
L_K	$\times 10^6$	-6.65(196)						-1008.(38)
l_J	$\times 10^{10}$							-1.201(89)
l_{JK}	$\times 10^9$		8.5258(10149)					41.86(965)
l_K	$\times 10^3$							1.7445(796)

Interaction Constants		$n = 0 \leftrightarrow 1, \tau = 3$	$n = 0 \leftrightarrow 1, \tau = 4$	$n = 1 \leftrightarrow 2, \tau = 3$	$n = 1 \leftrightarrow 2, \tau = 4$	$n = 2 \leftrightarrow 3, \tau = 3$ $n = 2 \leftrightarrow 3, \tau = 4$	$n = 2 \leftrightarrow \nu_3 = 1, n = 0, \tau = 4$
W		166.8582(162)	166.7758(136)	213.0773(5273)	207.0063(5832)	183.2(45) 171.2(46)	4.407(348)
W_J	$\times 10^3$	-2.76099(1287)	-0.41793(16541)				
W_K	$\times 10^1$	0.49415(464)	0.26507(2461)				
C						$n = 2, \tau = 3 \leftrightarrow \nu_3 = 1, n = 0, \tau = 4$ 320.38(21) $n = 2, \tau = 4 \leftrightarrow \nu_3 = 1, n = 0, \tau = 3$ 321.57(13)	

[a] All constants are in units of MHz except where indicated. The uncertainties in parenthesis are one standard deviation and refer to the least significant digits. Enough digits are supplied to reproduce the observed spectra.

[b] Constants without uncertainties were contained to the values reported by Ref. *2*.

[c] When only one value appears, the constants for the $\tau = 3$ and 4 torsional states were constrained to be equal.

~50% in the two analyses, link to levels in $n = 3$ in which there are no directly observed data.

IV. CONCLUSIONS

In this paper we have presented new mm/submm data for the rotation–torsion–vibration problem in the ground and $\upsilon_3 = 1$ vibrational states of HOOH. These data and our earlier mm/submm results are analyzed along with all other recent mm/submm, fir, and ir data in a single global analysis which fits all of these data to within their respective experimental uncertainties. Because of the strong Fermi and Coriolis couplings among the many states involved, such a global fit is required to optimally combine the information contents of the respective data. Because collectively these data are sensitive to the differences among the constants in the four τ sublevels, the number of separate states and spectral constants is large. This analysis has been done in the context of the generally available

TABLE 5
Statistical Summary of Data Sets Included in the Analysis

Type of Data	References	States[a]	Number of Data	Rms Deviation
Microwave, mm/submm-wave rotational-torsional transitions	1	$v = 0; n = 0,1$ $\tau = 1,2,3,4$	573	0.088 MHz
mm/submm-wave rotational-torsional transitions	-	$v_3 = 1, n = 0$ $\tau = 1,2,3,4$	148	0.103 MHz
submm-wave rotational-torsional transitions	-	$v = 0; n = 0,1$ $\tau = 1,2,3,4$	64	0.073 MHz
submm-wave rotational-torsional transitions	4	$v = 0; n = 0$ $\tau = 1,2,3,4$	61	0.060 MHz
ir energy levels	2	$v = 0, n = 0,1,2,3$ $v_3 = 1; n = 0,1$ $\tau = 1,2$	1473	0.00071 cm^{-1}
ir energy levels	2	$v = 0; n = 0,1,2,3$ $v_3 = 1; n = 0,1$ $\tau = 3,4$	1162	0.00047 cm^{-1}
ir combination differences	5	$v = 0; \tau = 1,2$	376	0.00068 cm^{-1}

[a] The ground vibrational state is denoted with $v = 0$.

asymmetric rotor fitting program CALFIT and is thus easily extendable as additional data are obtained.

V. ACKNOWLEDGMENTS

We would like to thank NASA and the Deutsche Forschungemeinschaft for the support of this work. F.C.D. and G.W. would also like to thank the Alexander von Humboldt Foundation for Max Plank Research Prizes.

REFERENCES

1. D. T. Petkie, T. M. Goyette, F. C. De Lucia, and P. Helminger, *J. Mol. Spectrosc.* **171,** 145–159 (1995).
2. C. Camy-Peyret, J.-M. Flaud, J. W. C. Johns, and M. Noel, *J. Mol. Spectrosc.* **155,** 84–104 (1992).
3. P. Helminger, W. C. Bowman, and F. C. De Lucia, *J. Mol. Spectrosc.* **85,** 120–130 (1981).
4. M. Bellini, E. Catacchini, P. De Natale, G. Di Lonardo, L. Fusina, M. Inguscio, and E. Venuti, *J. Mol. Spectrosc.* **177,** 115–123 (1996).
5. W. B. Olson, R. H. Hunt, B. W. Young, A. G. Maki, and J. W. Brault, *J. Mol. Spectrosc.* **127,** 12–34 (1988).
6. J.-M. Flaud, C. Camy-Peyret, J. W. C. Johns, and B. Carli, *J. Chem. Phys.* **91,** 1504–1510 (1989).
7. E. A. Cohen and H. M. Pickett, *J. Mol. Spectrosc.* **87,** 582–583 (1981).
8. W. C. Bowman, F. C. De Lucia, and P. Helminger, *J. Mol. Spectrosc.* **87,** 571–574 (1981).
9. R. A. Booker, R. L. Crownover, F. C. De Lucia, and P. Helminger, *J. Mol. Spectrosc.* **128,** 62–67 (1988).
10. G. Winnewisser, *Vib. Spectrosc.* **8,** 241–253 (1995).
11. H. M. Pickett, *J. Mol. Spectrosc.* **148,** 371–377 (1991).